Carbohydrate Polymers 99 (2014) 720–727

Contents lists available at ScienceDirect

Carbohydrate Polymers

journal homepage: www.elsevier.com/locate/carbpol

Synthesis and characterization of biotin modified cholesteryl pullulan as a novel anticancer drug carrier

Wenzhi Yang*, Miaomiao Wang, Lilan Ma, Haiying Li, Le Huang

College of Pharmacy & Key Laboratory of Pharmaceutical Quality Control of Hebei Province, Hebei University, Baoding 071002, China

ARTICLE INFO

Article history:
Received 6 April 2013
Received in revised form 5 September 2013
Accepted 5 September 2013
Available online 10 September 2013

Keywords:
Biotin-modified cholesteryl pullulan
Self-aggregated nanoparticle
Mitoxantrone
Drug delivery

ABSTRACT

A series of biotin modified cholesteryl pullulan (Bio-CHSP) conjugates with different degrees of substitution (DS) of biotin moiety were synthesized and characterized by Fourier transform infrared (FT-IR), proton nuclear magnetic resonance (^{1}H NMR) and X-ray diffraction (XRD). Bio-CHSP conjugates were amphiphilic in nature and their self-aggregation behavior in aqueous media was evaluated by the fluorescence probe technique. Bio-CHSP self-aggregated nanoparticles (Bio-CHSP NPs) were prepared and analyzed by dynamic light scattering (DLS), zeta potential and transmission electron microscopy (TEM) technologies. These novel nanoparticles were almost spherical in shape, and their size, ranging from 178.8 to 100.0 nm. The safety of Bio-CHSP NPs was studied through single dose toxicity test in mice, and the result showed that Bio-CHSP NPs were well tolerated at the intravenous dose of 200 mg/kg in mice. Moreover, as a model anticancer drug, mitoxantrone loaded Bio-CHSP NPs were also prepared and characterized in this study.

1. Introduction

Polymeric micelles self-aggregated from biocompatible and biodegradable polymers have attracted much attention due to their potential application in drug delivery (de Las Heras Alarcon, Pennadam, & Alexander, 2005; Li, Wang, Wang, Wang, & Jiang, 2013; Savić, Eisenberg, & Maysinger, 2006; Tong & Cheng, 2007). Polymeric amphiphiles consisting of hydrophilic and hydrophobic segments can form nanometer scale self-aggregates with a hydrophobic core and a hydrophilic shell due to the intramolecular and/or intermolecular interactions of hydrophobic segments in the aqueous media (Akiyoshi, Deguchi, Moriguchi, Yamaguchi, & Sunamoto, 1993; Kuroda, Fujimoto, Sunamoto, & Akiyoshi, 2002). Highly hydrated outer shells of the polymeric micelles can inhibit intermicellar aggregation of their hydrophobic inner cores. Thus, the self-aggregated nanoparticles are suitable for trapping hydrophobic drugs or some biomacromolecules such as proteins and genes to act as artificial molecular chaperones to improve their stability, control their release and intensify their bioactivity (Akiyoshi, Sasaki, & Sunamoto, 1999; Hirakura et al., 2010; Nomura, Ikeda, Yamaguchi, Aoyama, & Akiyoshi, 2003). Moreover, polymeric nanoparticles with targeting ligands, are promising candidates for cancer therapy, leading to a better therapeutic efficiency as well as reduced side effects (Blasi, Giovagnoli, Schoubben, Ricci, & Rossi, 2007; Nie, Xing, Kim, & Simons, 2007; Pulkkinen et al., 2008).

Recent studies revealed that biotin receptors were over expressed on numerous tumors characterized by rapid dividing and aggressive growth (Li, Lam, et al., 2013; Patel, Vadlapatla, Shah, & Mitra, 2012; Russell-Jones, McTavish, McEwan, Rice, & Nowotnik, 2004). For this reason, polymers that were bound with biotin tended to be uptaken by cancer cells and had higher distribution proportion in malignant tissues, compared to normal tissues (Heo et al., 2012; Kim, Cho, Lee, & Chu, 2007; Su, Chen, Cryns, & Messersmith, 2011; Xiong, Gong, Li, Li, & Guo, 2011). Na et al. (2003) synthesized vitamin H grafted pullulan acetate (BPA) and prepared the self-assembled nanoparticles as a targeted anti-cancer drug delivery system, the loading rhodamine B isothiocyanate (RITC)-labeled BPA nanoparticles exhibited very strong adsorption to the HepG2 cells, while the RITC-labeled PA nanoparticles did not show any significant interaction. Therefore, biotin act as the active tumor targeting ligand for various anti-cancer drugs, has the characteristics of special physicochemical and biological properties, including, low cytotoxicity and absence of antigenicity and immunogenicity, which enhances the intracellular uptake of drug within cancer cells (Bu et al., 2013; Kim et al., 2012).

The literature reported that drug loaded cholesterol-modified pullulan nanoparticles (CHSP NPs) coated with complexed human serum albumin molecules inhibited the drug release *in vitro* (Tao et al., 2012). CHSP NPs also showed a sustained release carrier for mitoxantrone *in vitro* (Yang et al., 2010). Although CHSP NPs has the excellent property of biocompatibility and shows a sustained

* Corresponding author. Tel.: +86 03125971107.
E-mail address: wenzhi_yang@sina.com (W. Yang).

0144-8617/$ – see front matter © 2013 Elsevier Ltd. All rights reserved.
http://dx.doi.org/10.1016/j.carbpol.2013.09.013

release carrier for mitoxantrone *in vitro*, it lacks active targeting to tumor tissues. Therefore, in this study, we synthesized biotin grafted CHSP copolymer, which focused on obtaining a tumor-targeted drug delivery carrier. The phisico-chemical characteristics of the Bio-CHSP were confirmed by FT-IR, ^{1}H NMR and XRD, and the biotin DS values were evaluated by ^{1}H NMR. The prepared amphiphilic pullulan composed of biotin and cholesterol grafts formed self-aggregated nanoparticles in aqueous media, and then the acute toxicity of Bio-CHSP NPs was assessed in mice. Furthermore, mitoxantrone (MTO) was chosen as a model drug to assess the potential of Bio-CHSP NPs as a carrier of anticancer drugs. As a dihydroxyanthracenedione anticancer agent, MTO has a wide range of antitumor activity and is used to treat various carcinomas. However, the therapy may cause some serious side effects such as nausea, vomiting, myelotoxicity, anemia, cardiotoxicity and immunosuppression (Hagemeister, Cabanillas, Coleman, Gregory, & Zinzani, 2005; Kroger et al., 2003; Neuhaus, Kieseier, & Hartung, 2006; Wundes, Kraft, Bowen, Gooley, & Nash, 2010; Yang & Morris, 2010; Zingler et al., 2005). Therefore, Bio-CHSP NPs being used as a carrier of MTO was hoped to sustain its release, enhance its therapeutic index and decrease its toxic effects in the future.

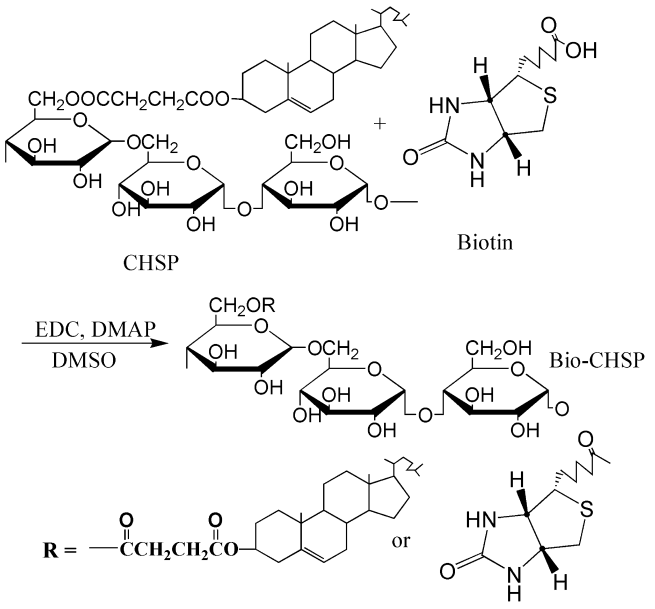

Fig. 1. The synthesis route of Bio-CHSP.

2. Materials and methods

2.1. Materials

Pullulan (Mw 200,000) was purchased from Hayashibara Tokyo (Japan). Biotin was provided by Sinopharm Chemical Reagent Co., Ltd. (Shanghai, China); 4-dimethylaminopyridine (DMAP) and 1-(3-dimethylaminopropyl)-3-ethylcarbodiimide hydrochloride (EDC·HCl) were purchased from Sigma Co. (MO, USA). Pyrene was supplied by Aldrich Co. (USA). Mitoxantrone was obtained from Beijing Xinze Science and Technology Co. (Beijing, China). Dialysis bags (Millipore molecular weight cut-off 8–14 KDa USA). Methanol, dichloromethane and ethanol were analytical grade and obtained from Kermel Chemical Reagent (Tianjin, China).

Six to eight-week-old male/female mice (20–24 g) were supplied by the Laboratory Animal Center of Hebei Medical University, (Hebei, China). The animals were acclimatized at a temperature of 25 ± 2 °C and a relative humidity of 70% ± 5% under natural light/dark conditions for at least 24 h before dosing. All the animal studies were approved by the center of Hebei Institutional Animal Care and Use Committee and performed in compliance with the Institutional Animal Care and Use Committee (IACUC) guidelines.

2.2. Synthesis of cholesteryl pullulan (CHSP) conjugates

The cholesteryl pullulan, with an average degree of substitution of 5.4 per 100 glucose units, was prepared by reacting pullulan with cholesterol succinate according to a procedure already reported (Yang et al., 2010), and the structure of CHSP is shown in Fig. 1.

2.3. Synthesis and characteristic of biotin modified CHSP (Bio-CHSP)

Cholesteryl pullulan (500 mg) was mixed with different amounts of biotin (753, 452 and 130 mg respectively), the mixture was completely dissolved in 6 mL dried DMSO by stirring, and then EDC (1.2 equiv biotin) and DMAP (0.1 equiv biotin) was added at 45 °C. After reaction for 5d, the mixture was cooled to room temperature and was precipitated in about 100 mL ethanol, filtered and washed with 50 mL dichloromethane, dilute alkali solution (50 mL, pH 11) and 50 mL anhydrous ethanol respectively, the obtained biotin graft polymer (Bio-CHSP) was dried in vacuum.

The chemical structure of Bio-CHSP was determined by FTIR-8400S spectroscopy (KBr pellets) (Shimadzu, Japan), and Avance III 600 MHz NMR spectrometer (Bruker, Switzerland) using DMSO-d_6 as the solvents at 600 MHz, and the characteristic of Bio-CHSP was also recorded with a D8 ADVACE X-ray diffractometer (Bruker, Switzerland)) to get X-ray powder diffraction diagrams. The degree of substitution (DS), defined as the number of the biotin moiety per 100 glucose units of Bio-CHSP, was determined by ^{1}H NMR.

2.4. Preparation of Bio-CHSP NPs

Bio-CHSP self-aggregated nanoparticles were prepared by dialysis method (Jeong et al., 2006; Wang et al., 2008). Briefly, Bio-CHSP (1 mg) was dissolved in 1 mL DMSO. To form nanoparticles, the solution was injected in dialysis bag to against 1000 mL deionized water and the dialyzed liquids were exchanged several times in 9 h followed by sonication using a probe type sonifier (SCIENTZ LCD JY 92-II, Ningbo) at 100 W for 2 min. The sonication step was repeated three times. The ice water bath and pulse (pulse on 2.0 s, pulse off 2.0 s) function were indispensable to protect the sample solution against heating built-up during the sonication. The solution of self-aggregated nanoparticles was filtered through a membrane filter (pore size: 0.45 μm, Millipore) to remove dust and then stored at 4 °C. The dialyzed solution was then analyzed or freeze-dried.

To observe the morphology of Bio-CHSP NPs sample, solutions (1 mg/mL) were dropped onto the carbon-coated 300 mesh copper grids. Then, the grids were air-dried and imaged using a transmission electron microscope (JEM-100C, JEOL, Japan). The particle size and zeta potential were determined by dynamic light scattering (Delsa^{TM} Nano zeta potentiometer, Beckman Coulter, USA).

2.5. Self-aggregation behavior of Bio-CHSP NPs

The self-aggregate property of Bio-CHSP conjugates and their critical aggregation concentration (cac) were estimated by the measurement of fluorescence spectroscopy (SANCO, 970-CRT, China) using pyrene as a hydrophobic probe (Wilhelm et al., 1991). To prepare sample solutions, a known amount of pyrene in methanol was added to each 10 mL test tubes and evaporated under a stream of nitrogen gas to remove the solvent. The amount was adjusted to give a pyrene concentration in the final solution of 6.0×10^{-7} M. Various concentrations (10 mL) of Bio-CHSP solutions were added

to each test tubes and they were sonicated for 30 min in an ultrasonic bath and shaken in a shaking air bath for 1 h at room temperature. The fluorescence excitation spectra were measured at an emission wavelength of 334 nm, and the emission spectra was recorded in the range of 350–500 nm. The excitation and emission bandwidths were 5 and 2 nm, respectively.

2.6. Preparation and characterization of the MTO-loaded Bio-CHSP NPs

MTO-loaded Bio-CHSP NPs were prepared by a dialysis method proposed by Jeong et al. (2006) and Kim et al. (2006). Briefly, MTO was dissolved in DMSO with different DS of Bio-CHSP and amount of triethylamine was added under stirring, and then the DMSO and free MTO were removed by dialyzing. The dialyzed liquids were exchanged each 1 h for the first 3 h and then each 2 h for another 6 h to against 1 L deionized water, followed by sonication using a probe type sonifier at 100 W for 2 min to obtain MTO-loaded Bio-CHSP self-aggregated nanoparticles. The MTO-loaded Bio-CHSP NPs were obtained after lyophillization through the LGJ-10 freezer-drier (Beijing Huaxing Technology Development Co., Ltd. Songyuan, China).

For the measurement of the drug loading content (LC) and drug loading efficiency (LE) (Yu, Li, Qiu, & Jin, 2008), a known amount of freeze-dried samples were dissolved by adding 1 mL distilled water and then 9 mL of DMSO to be adjusted to 10 mL. Empty Bio-CHSP NPs were used as the blank test. The drug loading contents and loading efficiency was estimated using UV spectrophotometer (8500, China) at wavelength of 625 nm, the LE and LC values can be calculated as following (1) and (2):

$$\mathrm{LE} = \frac{\text{The mass of MTO in the nanoparticles}}{\text{Total mass of MTO}} \times 100\% \quad (1)$$

$$\mathrm{LC} = \frac{\text{The mass of MTO in the nanoparticles}}{\text{The mass of nanoparticles weight}} \times 100\% \quad (2)$$

The morphology, zeta potential and particles size of MTO-loaded Bio-CHSP NPs were studied by the above methods in Section 2.4. X-ray powder diffraction diagrams were also recorded to identify MTO-loaded Bio-CHSP NPs.

2.7. MTO release behavior from Bio-CHSP NPs in vitro

MTO release behavior was studied *in vitro* by dialysis method in phosphate buffered saline (PBS, 0.1 M; pH 7.4, 6.8 and 3.5). Then the solution of MTO-loaded Bio-CHSP NPs (1 mg/mL) was placed into dialysis bags and dialyzed against the release media at 37 ± 0.2 °C in an air-bath shaker at 100 rpm. At predetermined time intervals, the release medium was collected and the fresh release media was added. The released amount of MTO was determined by UV spectrophotometer at 609 nm. The accumulative release percentage ($Q\%$) was calculated by the following equation, and all experiments were carried out in triplicate.

$$Q\% = \frac{Cn \times V + Vi\sum_{i=0}^{i=n} Ci}{W\mathrm{Drug-Bio-CHSP-nanoparticles} \times \mathrm{Drugloading}} \times 100\% \quad (3)$$

where C_n is the sample concentration at T_n, V is the total volume of release medium, V_i is the sample volume at T_i, C_i is the sample concentration at T_i (both V_0 and C_0 were equal to zero), and T_n is sampling at the N_{th} time.

2.8. In vivo toxicity

The toxicity of Bio-CHSP NPs was evaluated *in vivo* according to the previous reported method (Tang et al., 2010; Zhang et al., 2012). Adult male and female ICR mice (20–24 g) were randomly divided equally into two groups, each with 10 mice. The experimental group received a single intravenous (*i.v.*) dose of blank Bio-CHSPNs (200 mg/kg), the control group was treated with a single *i.v.* dose of same amount of normal saline to make a comparison keeping similar environment. All animals were fed with normal diet, and water was provided *ad libitum*. Animals were observed carefully for the onset of any signs of toxicity and monitored for changes in food intake and body weight at 1, 8, and 15 days. After being sacrificed at 15 days, internal organs of each animal were harvested and observed grossly. The histological changes, such as acute-chronic inflammatory symptoms, fibroblastic proliferation, and any other inflammation symptoms were observed. For further histological examinations, specimens of major organs such as heart, liver, spleen, lung, and kidney were fixed in 10% phosphate buffered formalin, embedded in paraffin, sectioned, and stained with hematoxylin and eosin (H&E).

2.9. Statistical analysis

Statistical analysis was conducted by using the Student's *t*-test with $p < 0.05$ as a significant difference. The experimental results are given in the format of (mean ± SD) in table.

3. Results and discussion

3.1. Synthesis and characterization of Bio-CHSP

Cholesteryl grafted pullulan (CHSP) have been synthesized according to our reported (Yang et al., 2010). Moreover, Bio-CHSP was synthesized by the esterification reaction and the synthetic route has been shown in Fig. 1. The reaction between CHSP and biotin was catalyzed by DMAP/EDC in one step. Biotin was coupled to the hydroxyl group of CHSP using coupling agent and various Bio-CHSP conjugates with different biotin DS values were synthesized by controlling the mole ratio of biotin and CHSP.

Fig. 2 shows the FT-IR spectra of CHSP (2a), Bio-CHSP (2b) and biotin (2c). Compared with CHSP, the peaks of Bio-CHSP (Fig. 2b), such as O—H stretch overlapped with =N—H stretch at 3500–3200 cm^{-1}, stretching vibration band relative to —CH_3, —CH_2— groups at about 2924 cm^{-1} and the stretching vibration of the C=O bonds at about 1730 cm^{-1}, have significantly enhanced. Furthermore, the peaks of amide I band at about 1685 cm^{-1}, amide II band at about 1536 cm^{-1} and amide III band at about 1266 cm^{-1} can be observed. The infrared absorption characteristic peaks suggest that there should be existence of ester, methylene and amide group, which confirmed biotin was successfully reacted with CHSP by esterification.

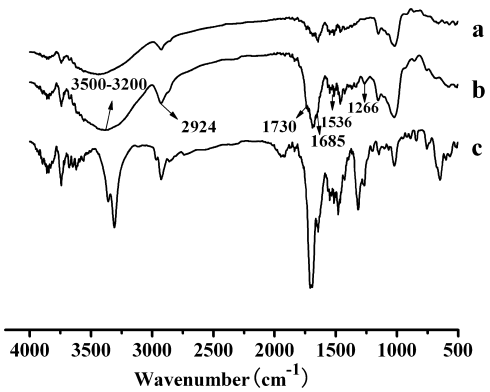

Fig. 2. IR spectra of (a) CHSP, (b) Bio-CHSP and (c) Biotin.

Table 1
The characterization of blank Bio-CHSP NPs and MTO-loaded Bio-CHSP NPs.

Sample-$_{DS}$ [a]	D/C (w/w)[b]	D_h (nm)[c]	PI[c]	LE (%)[d]	LC (%)[e]	ζ (mv)[f]
Bio-CHSP$_{-20.1}$	0	178.8 ± 4.3	0.211 ± 0.015	–	–	−4.12
	1/10	205.0 ± 3.4	0.260 ± 0.021	80.4 ± 6.2	7.2 ± 0.56	−2.95
Bio-CHSP$_{-29.2}$	0	135.2 ± 2.6	0.163 ± 0.018	–	–	−10.16
	1/5	172.8 ± 3.1	0.174 ± 0.013	80.0 ± 5.5	14.4 ± 1.00	−1.69
	1/10	168.3 ± 2.5	0.165 ± 0.018	85.2 ± 5.2	7.8 ± 0.48	−0.62
	1/15	171.7 ± 1.8	0.137 ± 0.024	89.1 ± 7.4	6.3 ± 0.83	−0.98
Bio-CHSP$_{-38.9}$	0	100.0 ± 3.2	0.148 ± 0.026	–	–	−13.92
	1/10	146.3 ± 6.2	0.204 ± 0.016	53.6 ± 6.2	4.8 ± 0.55	−1.12

[a] The DS values of biotin per hundred glucose units, determined by ^{1}H NMR.
[b] The weight of drug and carrier (MTO/Bio-CHSP) self-aggregated nanoparticles (mg/mg).
[c] The size and size distribution (mean value ± S.D.) determined by the DLS in distilled water with three times.
[d] (Loading MTO/total MTO) × 100% determined by UV–vis spectrophotometer at 625 nm.
[e] (Loading MTO/Bio-CHSP self-aggregated nanoparticles) × 100% determined by UV–vis spectrophotometer at 625 nm.
[f] The zeta potential of blank Bio-CHSP NPs/or MTO-loaded Bio-CHSP NPs in distilled water at 1 mg/mL.

Fig. 3 shows the ^{1}H NMR spectra of biotin (3a), CHSP (3b) and Bio-CHSP (3c). The CHSP ^{1}H NMR spectrum permitted the identification of the protons: 0.59–1.20 ppm (the H signal of cholesterol) (Kim et al., 2012; Zipser, Bradford, & Hollingsworth, 1998), the singlet at 0.65 and 0.97 ppm which is assigned to the two angular methyl groups (18-C***H***$_3$ and 19-C***H***$_3$), the peak at 0.84 ppm (26, 27-C***H***$_3$), the peak at 0.90 ppm (21-C***H***$_3$), 2.50 (DMSO-d_6) and 2.55 (2 methylene groups, —OCC***H***$_2$C***H***$_2$CO—) ppm. The peak at 2.55 ppm is the proton signal of two methylene groups (—OCC***H***$_2$C***H***$_2$CO—), this peak plays a key role on supporting the conclusion that pullulan was successfully reacted with cholesterol by succinic acid linker. Moreover, the degree of substitute (DS) of cholesterol residues per 100 glucose units in pullulan could be calculated by the ratio of methylene groups protons (2.55 ppm) to sugar protons (C_1 position of α-1,6 and α-1,4 glycosidic bonds, 4.65 and 5.05 ppm (Sivakumar & Panduranga Rao, 2003; Yang et al., 2010). As shown in Fig. 3c, compared with CHSP, the new peaks of Bio-CHSP appeared, such as 1.20–1.80 ppm (***a***, 6H, —(C***H***$_2$)$_3$—, m), 2.34 ppm (***b***, 2H, brs), 2.60 ppm (***c***, 1H, d), 2.84 ppm (***c***, 1H, d), 3.10 ppm (***d***, 1H, brs), 4.17 ppm (***e***, 1H, dd), 4.32 ppm (***f***, 1H, m) and 6.45 ppm (***g***, 2H, =N—H, brs) (Chen et al., 2005; Iwasaki & Akiyoshi, 2006; Kim et al., 2007; Tong, Yao, Li, & Han., 2006), which confirmed biotin has been grafted onto CHSP backbone successfully. Moreover, the ^{1}H NMR peaks of biotin and cholesterol do not appear in the range of 4.5–5.3 ppm. If ^{1}H NMR signal appears in this area, it belongs to pullulan. Therefore, the DS of the biotin moiety, could be calculated by comparing the ratio of methine of biotin protons (4.17 and 4.32 ppm) to protons (C_1 position of α-1,6 and α-1,4 glycosidic bonds, 4.65 and 5.05 ppm). The degree of substitution (DS) of biotin moiety could be determined as follows:

$$\mathrm{DS} = \frac{(A\delta 4.17 + A\delta 4.32)}{2(A\delta 4.65 + A\delta 5.05)} \times 100$$

The results of DS of biotin moiety are shown in Table 1.

In order to prove that Bio-CHSP was successfully synthesized by covalent bond, the grafted polysaccharide was further characterized by XRD. The XRD result (figure not shown) shows biotin has eight typical crystal peaks at 2θ of 8.4, 12.1, 17.7, 18.8, 21.3, 22.5, 28.5, 34.1° and numerous small peaks between 35 and 60°. CHSP has a broad peak at 2θ of 17.8°. The mixture of biotin and Bio-CHSP (the ratio 10:1, w/w) shows biotin crystal peaks. However, the Bio-CHSP only shows broad diffraction peak at 2θ of 18.9°, which indicates the crystalline structure of biotin has been disrupted after chemical modification. The above results also confirm that Bio-CHSP is synthesized, and these results are similar to chemically modified pullulan (Jung, Jeong, & Kim, 2003; Kim & Oh, 2010).

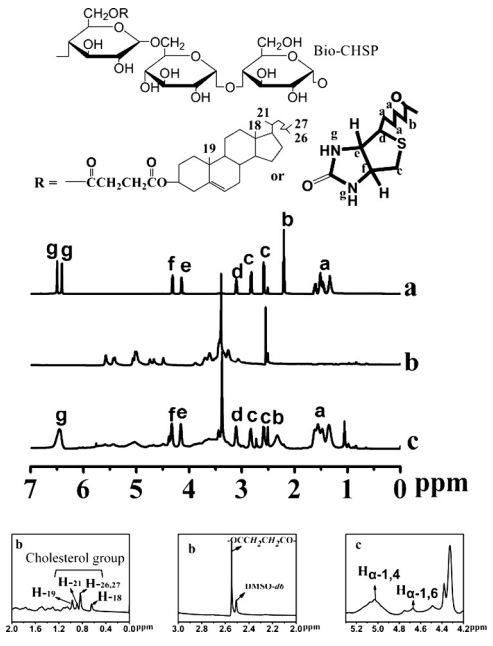

Fig. 3. The ^{1}H NMR spectra of (a) Biotin, (b) CHSP and (c) Bio-CHSP.

3.2. Self-aggregation behavior of Bio-CHSP NPs

Amphiphilic block or graft polymers can show self-aggregation potential in aqueous media (Akiyoshi, Deguchi, Tajima, Nishikawa, & Sunamoto, 1997). To evaluate the self-aggregation behavior of Bio-CHSP, fluorescence spectroscopy was performed and pyrene was used as a hydrophobic probe (Colombani et al., 2007). The fluorescence intensity of pyrene was found to increase with the increasing concentration of Bio-CHSP, which implied Bio-CHSP molecules self-aggregated in water and the pyrene could preferentially transfer itself from the aqueous phase to these hydrophobic micro-domains. This trend in fluorescence spectra was similar to those previously reported for other polymeric amphiphiles (Jung, Jeong, Kim, & Kim, 2004; Wang, Liu, Jiang, & Zhang, 2007).

The critical aggregation concentration (cac) can be determined from the change of the I_{372}/I_{383} value of the pyrene in presence of the different concentration of amphiphile copolymer (Binana-Limbele & Zana, 1987; Chang et al., 2000). The cac values of Bio-CHSP$_{-20.1}$, Bio-CHSP$_{-29.2}$ and Bio-CHSP$_{-38.9}$ were 0.0055, 0.0017 and 0.00015 mg/mL, respectively. The results show the cac value of Bio-CHSP decreased with increase in DS. The reason for this phenomenon could be that the increased level of hydrophobic attachment would result in the high stability of the polymer micelles and the polarity of the medium induces an increasing value of the I_{372}/I_{383}, which agrees with the idea that Li and Kwon

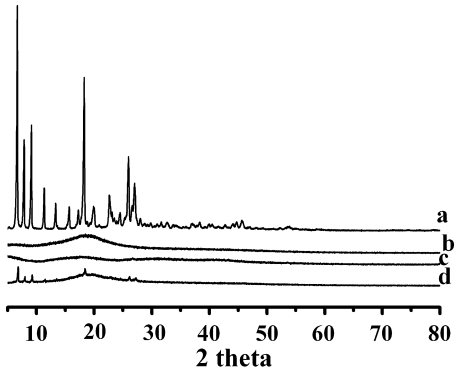

Fig. 4. The X-ray powder diffractions of (a) MTO, (b) Bio-CHSP, (c) MTO-loaded Bio-CHSP and (d) the physical mixture of a and b (the ratio 1:10, w/w).

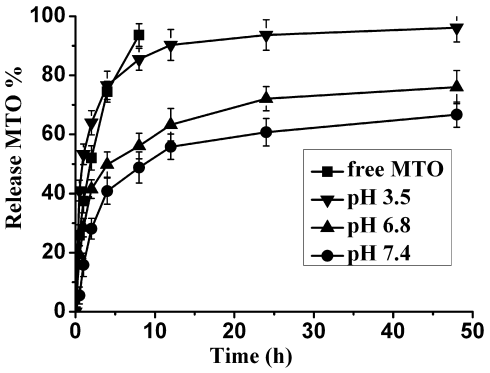

Fig. 6. MTO release from Bio-CHSP$_{-29.2}$ NPs with a drug loading content of 7.8% at 37 °C in (-■-) free MTO in PBS buffer (pH 7.4), (-▼-) acetate buffer (pH 3.5), (-▲-) PBS buffer (pH 6.8) and (-●-) PBS buffer (pH 7.4).

proposed (Li & Kwon, 2000). It could be deduced from the cac of Bio-CHSP nanoparticles that the aggregation of Bio-CHSP molecules in aqueous media was due to the hydrophobicity of the biotin and cholesterol moieties.

3.3. Characterization of Bio-CHSP and MTO-loaded Bio-CHSP NPs

To further confirm the MTO-loaded Bio-CHSP NPs successfully prepared, the X-ray diffraction spectra of the MTO-loaded Bio-CHSP is shown in Fig. 4. It can be observed that the XRD patterns show broad peaks in the Bio-CHSP (Fig. 4b) and sharp peaks in MTO drug crystals (Fig. 4a). In addition, specific drug crystal peaks are observed in the physical mixture of MTO and Bio-CHSP (Fig. 4d), whereas specific peaks of drug crystals are disappeared in the MTO-loaded Bio-CHSP (Fig. 4c). It is known that a crystalline drug shows sharp, specific, crystal peaks when it exists as drug crystals, but in this case, the drug exists as a molecular dispersion within the nanoparticles. These results show that the MTO is successfully entrapped into the nanoparticles as a molecular dispersion (Guyot & Fawaz, 1998; Jung et al., 2004; Li, Xu, et al., 2013).

Fig. 5 shows the morphology and size of the blank and MTO-loaded Bio-CHSP NPs by TEM and DLS respectively. The results are shown in Table 1. TEM images (Fig. 5a and b) shows that Bio-CHSP$_{-29.2}$ and MTO-loaded Bio-CHSP$_{-29.2}$ NPs are almost spherical in shape. The size of Bio-CHSP$_{-29.2}$ and MTO-loaded Bio-CHSP$_{-29.2}$ NPs, is around 90 nm and 140 nm appeared by TEM, whereas 135.2 ± 2.6 nm and 168.3 ± 2.5 nm determined by DLS respectively,

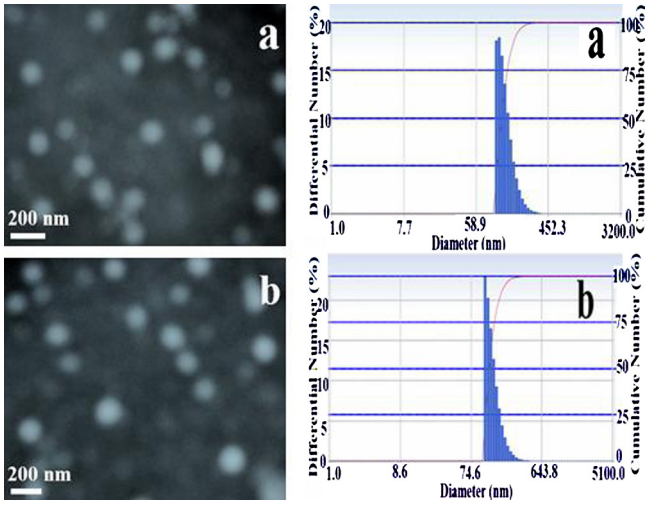

Fig. 5. TEM image and size distribution of (a) Bio-CHSP$_{-29.2}$ NPs and (b) MTO-loaded Bio-CHSP$_{-29.2}$ NPs.

which is slightly smaller than that measured by DLS. The results are mainly due to the different preparation process of the sample. DLS determines the size in the hydrated state of the sample, whereas TEM depicts the size in the dried state of the sample (Liu, Desai, Chen, & Park, 2004; Wang et al., 2007). Table 1 summarizes the characteristics of Bio-CHSP and MTO-loaded Bio-CHSP NPs. The mean diameters of Bio-CHSP NPs determined by DLS are in the range of 100–180 nm depending on biotin DS value. The size of nanoparticles decreased with DS of biotin moiety increasing, because the more hydrophobic groups are beneficial to form more compact hydrophobic cores (Chen et al., 2011; Nishikawa, Akiyoshi, & Sunamoto, 1996). The zeta potentials of Bio-CHSP NPs with different DS of biotin moiety are obvious slight negative in distilled water. MTO loading capacity increased from 6.3% to 14.4% with the weight ratio of MTO to Bio-CHSP$_{-29.2}$ increasing from 1/15 to 1/5, but loading efficiency decreased from 89.1% to 80% at the same time. Thus, the optimal weight ratio 1/10 based on the drug loading properties, was selected to prepare MTO-loaded Bio-CHSP NPs.

These results have verified that Bio-CHSP can form nanoparticles in the aqueous environment because the polymeric nanoparticles have the hydrophilic shell of pullulan backbone and the hydrophobic core of biotin and cholesterol moieties, and it can form the non-covalently cross-linked structure by the hydrophobic association of biotin and cholesterol moieties, and this unique supramolecular structure is suitable for trapping the hydrophobic drugs (Kumar, Muzzarelli, Muzzarelli, Sashiwa, & Domb, 2004; Wang et al., 2007).

3.4. In vitro drug release study

To study the drug release behavior, MTO-loaded Bio-CHSP NPs *in vitro* was carried out in PBS (pH 7.4, 6.8 and 3.5) at 37 °C. As shown in Fig. 6, it was observed that the release of MTO from MTO-loaded Bio-CHSP$_{-29.2}$ NPs with loading content 7.8% evidenced some slight pH-dependent behavior, which exhibited an obvious decrease in the release rate with the increasing pH of the release medium. Moreover, similar release characteristics were observed for the other drug loading contents (data not shown). It is known that the release rate of a drug incorporated in a hydrophobic domain depends on the solubility and diffusivity of the drug (Na, Park, Kim, & Bae, 2000). The lower pH lead to obtaining more phosphate type of MTO which belongs to easily dissolved state, the increasing solubility of MTO in the nanoparticles induces easier drug release. Therefore, MTO released from Bio-CHSP NPs much faster in PBS of pH 3.5 than that of pH 7.4. Moreover, the release behavior of free MTO and MTO-loaded Bio-CHSP NPs *in vitro* was carried out in PBS (pH 7.4) at 37 °C. In PBS (pH 7.4), the free MTO released

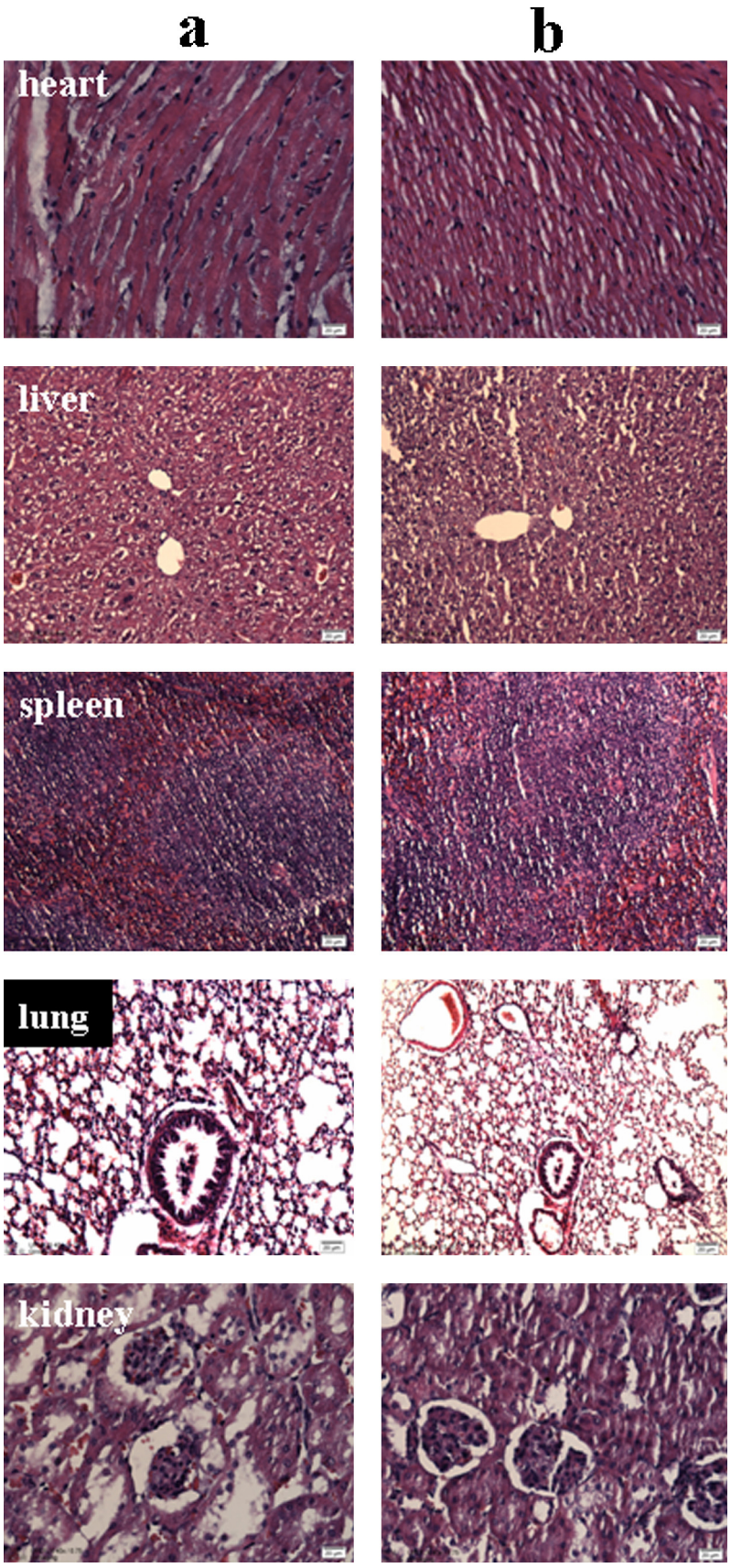

Fig. 7. Representative photomicrographs of the heart, liver, spleen, lung, and kidney sections (H&E staining) of mice of control group (a) and treated with test Bio-CHSP NPs (b).

more than 90% within 8 h. However, in the MTO-loaded Bio-CHSP NPs, MTO appeared to be released in a biphasic way, and the release profiles show the release behavior of MTO from Bio-CHSP NPs is initially rapid and then slow after 12 h. The initial burst of MTO from nanoparticles suggests some part of the drug is absorbed onto the surface of nanoparticles since adsorbed drug instantaneously dissolved when it contacted the release medium, whereas following slow and uniform release of MTO could be due to the diffusion of the entrapped drug in nanoparticles (Chen et al., 2011). It is obviously showed that MTO is slightly sustained releasing from Bio-CHSP nanoparticles in pH 7.4 release medium for 48 h, which suggests Bio-CHSP NPs have a potential as a sustained release carrier for MTO.

3.5. *In vivo* toxicity of Bio-CHSP NPs

To demonstrate the safety of Bio-CHSP NPs as a drug carrier, the acute toxicity *in vivo* experiment was studied. All the mice were healthy throughout the experiment period, as judged from the body weight data, food intake data and pathological changes of mice during the experiment. No significant differences between the Bio-CHSP NPs group and the control group in clinical signs, *e.g.* diarrhea, fever, and other systemic symptoms, and no mortality occurred throughout the entire study course. The data of the body weight and food intake for both male and female mice between the two studied groups are also not shown significant difference. Animals were sacrificed for histopathological study on 15th, Fig. 7 shows microscopic examination of the representative histopathological of major organs including heart, liver, spleen, lung, and kidney sections stained with H&E. On all accounts, no significant histological differences are observed between control and Bio-CHSP NPs administered tissue samples. All the above results indicated that no apparent acute toxicity of the Bio-CHSP NPs was found in the experimental animals after *i.v.* at a dose of 200 mg/kg. Thus, histopathological studies confirmed that Bio-CHSP NPs is safe and biocompatible for use in drug delivery systems.

4. Conclusions

Novel self-aggregated nanoparticles were prepared from polymeric amphiphiles, biotin modified cholesteryl pullulan (Bio-CHSP) conjugates, and the relationships between the chemical structure, the amphiphilic property and the morphological characteristics of Bio-CHSP NPs were investigated in this study. The formation of Bio-CHSP NPs is due to the hydrophobic interactions of biotin and cholesterol moieties in aqueous media, and the acute toxicity experiment *in vivo* shows that Bio-CHSP *i.v.* administration (at dose of 200 mg/kg) is safe for use in drug delivery systems. The drug loading and release experiments show that Bio-CHSP NPs can be used as a carrier for mitoxantrone. This novel nanoparticle system may be useful in the target delivery of hydrophobic drugs for cancer therapeutics, and the further investigations are in progress.

Acknowledgements

This work was supported by the Natural Science Foundation of Hebei Province (No. H2012201069) and the Natural Science Foundation of Hebei University, China (No. 2010-193).

References

Akiyoshi, K., Deguchi, S., Moriguchi, N., Yamaguchi, S., & Sunamoto, J. (1993). Self-aggregates of hydrophobized polysaccharides in water. Formation and characteristics of nanoparticles. *Macromolecules*, *26*(12), 3062–3068.

Akiyoshi, K., Deguchi, S., Tajima, H., Nishikawa, T., & Sunamoto, J. (1997). Microscopic structure and thermoresponsiveness of a hydrogel nanoparticle by self-assembly of a hydrophobized polysaccharide. *Macromolecules*, *30*(4), 857–861.

Akiyoshi, K., Sasaki, Y., & Sunamoto, J. (1999). Molecular chaperone-like activity of hydrogel nanoparticles of hydrophobized pullulan: Thermal stabilization with refolding of carbonic anhydrase B. *Bioconjugate Chemistry*, *10*(3), 321–324.

Binana-Limbele, W., & Zana, R. (1987). Fluorescence probing of microdomains in aqueous solutions of polysoaps. 1. Use of pyrene to study the conformational state of polysoaps and their comicellization with cationic surfactants. *Macromolecules*, *20*(6), 1331–1335.

Blasi, P., Giovagnoli, S., Schoubben, A., Ricci, M., & Rossi, C. (2007). Solid lipid nanoparticles for targeted brain drug delivery. *Advanced Drug Delivery Reviews*, *59*(6), 454–477.

Bu, L., Gan, L. C., Guo, X. Q., Chen, F. Z., Song, Q., Zhao, Q., et al. (2013). Trans-resveratrol loaded chitosan nanoparticles modified with biotin and avidin to target hepatic carcinoma. *International Journal of Pharmaceutics*, *452*(1/2), 355–362.

Chang, Y., Lee, S. C., Kim, K. T., Kim, C., Reeves, S. D., & Allcock, H. R. (2000). Synthesis and micellar characterization of an amphiphilic diblock copolyphosphazene. *Macromolecules*, *34*(2), 269–274.

Chen, F. E., Jia, H. Q., Chen, X. X., Dai, H. F., Xie, B., Kuang, Y. Y., et al. (2005). Synthetic studies on d-biotin, Part 9. An improved asymmetric synthetic route to d-biotin via hoffmann-roche lactone-thiolactone approach. *Chemical and Pharmaceutical Bulletin*, *53*(7), 743–746.

Chen, M. M., Liu, Y., Yang, W. Z., Li, X. M., Liu, L. R., Zhou, Z. M., et al. (2011). Preparation and characterization of self-assembled nanoparticles of 6-O-cholesterol-modified chitosan for drug delivery. *Carbohydrate Polymers*, *84*(4), 1244–1251.

Colombani, O., Ruppel, M., Schubert, F., Zettl, H., Pergushov, D. V., & Muller, A. H. E. (2007). Synthesis of poly(n-butyl acrylate)-block-poly(acrylic acid) diblock copolymers by ATRP and their micellization in water. *Macromolecules*, *40*(12), 4338–4350.

de Las Heras Alarcon, C., Pennadam, S., & Alexander, C. (2005). Stimuli responsive polymers for biomedical applications. *Chemical Society Reviews*, *34*(3), 276–285.

Guyot, M., & Fawaz, F. (1998). Nifedipine loaded-polymeric microspheres: Preparation and physical characteristics. *International Journal of Pharmaceutics*, *175*(1), 61–74.

Hagemeister, F., Cabanillas, F., Coleman, M., Gregory, S. A., & Zinzani, P. L. (2005). The role of mitoxantrone in the treatment of indolent lymphomas. *The Oncologist*, *10*(2), 150–159.

Heo, D. N., Yang, D. H., Moon, H. J., Lee, J. B., Bae, M. S., Lee, S. C., et al. (2012). Gold nanoparticles surface-functionalized with paclitaxel drug and biotin receptor as theranostic agents for cancer therapy. *Biomaterials*, *33*(3), 856–866.

Hirakura, T., Yasugi, K., Nemoto, T., Sato, M., Shimoboji, T., Aso, Y., et al. (2010). Hybrid hyaluronan hydrogel encapsulating nanogel as a protein nanocarrier: New system for sustained delivery of protein with a chaperone-like function. *Journal of Controlled Release*, *142*(3), 483–489.

Iwasaki, Y., & Akiyoshi, K. (2006). Synthesis and characterization of amphiphilic polyphosphates with hydrophilic graft chains and cholesteryl groups as nanocarriers. *Biomacromolecules*, *7*(5), 1433–1438.

Jeong, Y. I., Kim, S. H., Jung, T. Y., Kim, I. Y., Kang, S. S., Jin, Y. H., et al. (2006). Polyion complex micelles composed of all-trans retinoic acid and poly (ethylene glycol)-grafted-chitosan. *Journal of Pharmaceutical Sciences*, *95*(11), 2348–2360.

Jung, S. W., Jeong, Y. I., & Kim, S. H. (2003). Characterization of hydrophobized pullulan with various hydrophobicities. *International Journal of Pharmaceutics*, *254*(2), 109–121.

Jung, S. W., Jeong, Y. I., Kim, Y. H., & Kim, S. H. (2004). Self-assembled polymeric nanoparticles of poly(ethylene glycol) grafted pullulan acetate as a novel drug carrier. *Archives of Pharmacal Research*, *27*(5), 562–569.

Kim, S., Cho, S., Lee, Y., & Chu, L. Y. (2007). Biotin-conjugated block copolymeric nanoparticles as tumor-targeted drug delivery systems. *Macromolecular Research*, *15*(7), 646–655.

Kim, J. H., Kim, Y. S., Kim, S., Park, J. H., Kim, K., Choi, K., et al. (2006). Hydrophobically modified glycol chitosan nanoparticles as carriers for paclitaxel. *Journal of Controlled Release*, *111*(1/2), 228–234.

Kim, J. H., Li, Y., Kim, M. S., Kang, S. W., Jeong, J. H., & Lee, D. S. (2012). Synthesis and evaluation of biotin-conjugated pH-responsive polymeric micelles as drug carriers. *International Journal of Pharmaceutics*, *427*(2), 435–442.

Kim, I. S., & Oh, I. J. (2010). Preparation and characterization of stearic acid-pullulan nanoparticles. *Archives of Pharmacal Research*, *33*(5), 761–767.

Kroger, N., Damon, L., Zander, A. R., Wandt, H., Derigs, G., Ferrante, P., et al. (2003). Secondary acute leukemia following mitoxantrone-based high-dose chemotherapy for primary breast cancer patients. *Bone Marrow Transplantation*, *32*(12), 1153–1157.

Kumar, M. N. V. R., Muzzarelli, R. A. A., Muzzarelli, C., Sashiwa, H., & Domb, A. J. (2004). Chitosan chemistry and pharmaceutical perspectives. *Chemical Reviews*, *104*(12), 6017–6084.

Kuroda, K., Fujimoto, K., Sunamoto, J., & Akiyoshi, K. (2002). Hierarchical self-assembly of hydrophobically modified pullulan in water: Gelation by networks of nanoparticles. *Langmuir*, *18*(10), 3780–3786.

Li, Y., & Kwon, G. (2000). Methotrexate esters of poly(ethylene oxide)-block -poly(2-hydroxyethyl-L-aspartamide). Part I: Effects of the level of methotrexate conjugation on the stability of micelles and on drug release. *Pharmaceutical Research*, *17*(5), 607–611.

Li, M., Lam, J. W. Y., Mahtab, F., Chen, S. J., Zhang, W. J., Hong, Y. N., et al. (2013). Biotin-decorated fluorescent silica nanoparticles with aggregation-induced emission characteristics: Fabrication, cytotoxicity and biological applications. *Journal of Materials Chemistry B*, *1*(5), 676–684.

Li, B. G., Wang, Q., Wang, X., Wang, C. Z., & Jiang, X. Q. (2013). Preparation, drug release and cellular uptake of doxorubicin-loaded dextran-b-poly(ε-caprolactone) nanoparticles. *Carbohydrate Polymers*, *93*(2), 430–437.

Li, Y. G., Xu, X. F., Shen, Y. Y., Qian, C. Y., Lu, F., & Guo, S. R. (2013). Preparation and evaluation of copolymeric micelles with high paclitaxel contents and sustained drug release. *Colloids and Surfaces A: Physicochemical and Engineering Aspects*, *429*(0), 12–18.

Liu, C. G., Desai, K. G. H., Chen, X. G., & Park, H. J. (2004). Linolenic Acid-modified chitosan for formation of self-assembled nanoparticles. *Journal of Agricultural and Food Chemistry*, *53*(2), 437–441.

Na, K., Bum Lee, T., Park, K. H., Shin, E. K., Lee, Y. B., & Choi, H. K. (2003). Self-assembled nanoparticles of hydrophobically-modified polysaccharide bearing vitamin H as a targeted anti-cancer drug delivery system. *European Journal of Pharmaceutical Sciences*, *18*(2), 165–173.

Na, K., Park, K. H., Kim, S. W., & Bae, Y. H. (2000). Self-assembled hydrogel nanoparticles from curdlan derivatives: Characterization, anti-cancer drug release and interaction with a hepatoma cell line (HepG2). *Journal of Controlled Release*, *69*(2), 225–236.

Neuhaus, O., Kieseier, B. C., & Hartung, H. P. (2006). Therapeutic role of mitoxantrone in multiple sclerosis. *Pharmacology and Therapeutics*, *109*(1/2), 198–209.

Nie, S., Xing, Y., Kim, G. J., & Simons, J. W. (2007). Nanotechnology applications in cancer. *Annual Review of Biomedical Engineering*, *9*(1), 257–288.

Nishikawa, T., Akiyoshi, K., & Sunamoto, J. (1996). Macromolecular complexation between bovine serum albumin and the self-assembled hydrogel nanoparticle of hydrophobized polysaccharides. *Journal of the American Chemical Society*, *118*(26), 6110–6115.

Nomura, Y., Ikeda, M., Yamaguchi, N., Aoyama, Y., & Akiyoshi, K. (2003). Protein refolding assisted by self-assembled nanogels as novel artificial molecular chaperone. *FEBS Letters*, *553*(3), 271–276.

Patel, M., Vadlapatla, R. K., Shah, S., & Mitra, A. K. (2012). Molecular expression and functional activity of sodium dependent multivitamin transporter in human prostate cancer cells. *International Journal of Pharmaceutics*, *436*(1/2), 324–331.

Pulkkinen, M., Pikkarainen, J., Wirth, T., Tarvainen, T., Haapa-aho, V., Korhonen, H., et al. (2008). Three-step tumor targeting of paclitaxel using biotinylated PLA-PEG nanoparticles and avidin–biotin technology: Formulation development and in vitro anticancer activity. *European Journal of Pharmaceutics and Biopharmaceutics*, *70*(1), 66–74.

Russell-Jones, G., McTavish, K., McEwan, J., Rice, J., & Nowotnik, D. (2004). Vitamin-mediated targeting as a potential mechanism to increase drug uptake by tumours. *Journal of Inorganic Biochemistry*, *98*(10), 1625–1633.

Savić, R., Eisenberg, A., & Maysinger, D. (2006). Block copolymer micelles as delivery vehicles of hydrophobic drugs: Micelle–cell interactions. *Journal of Drug Targeting*, *14*(6), 343–355.

Sivakumar, P. A., & Panduranga Rao, K. (2003). The use of cholesteryl pullulan for the preparation of stable vincristine liposomes. *Carbohydrate Polymers*, *51*(3), 327–332.

Su, J., Chen, F., Cryns, V. L., & Messersmith, P. B. (2011). Catechol polymers for pH-responsive, targeted drug delivery to cancer cells. *Journal of the American Chemical Society*, *133*(31), 11850–11853.

Tang, H. B., Li, L., Chen, H., Zhou, Z. M., Chen, H. L., Li, X. M., et al. (2010). Stability and in vivo evaluation of pullulan acetate as a drug nanocarrier. *Drug Delivery*, *17*(7), 552–558.

Tao, X. J., Zhang, Q. F., Ling, K., Chen, Y. C., Yang, W. Z., Gao, F. F., et al. (2012). Effect of pullulan nanoparticle surface charges on HSA complexation and drug release behavior of HSA-bound nanoparticles. *PloS one*, *7*(11), e49304.

Tong, R., & Cheng, J. (2007). Anticancer polymeric nanomedicines. *Polymer Reviews*, *47*(3), 345–381.

Tong, D., Yao, J., Li, H., & Han, S. (2006). Synthesis and characterization of thermo- and pH-sensitive block copolymers bearing a biotin group at the poly(ethylene oxide) chain end. *Journal of Applied Polymer Science*, *102*, 3552–3558.

Wang, Y. S., Jiang, Q., Li, R. S., Liu, L. L., Zhang, Q. Q., & Zhao, J. (2008). Self-assembled nanoparticles of cholesterol-modified O-carboxymethyl chitosan as a novel carrier for paclitaxel. *Nanotechnology*, *19*(14), 145101.

Wang, Y. S., Liu, L. R., Jiang, Q., & Zhang, Q. Q. (2007). Self-aggregated nanoparticles of cholesterol-modified chitosan conjugate as a novel carrier of epirubicin. *European Polymer Journal*, *43*(1), 43–51.

Wilhelm, M., Zhao, C. L., Wang, Y., Xu, R., Winnik, M. A., Mura, J. L., et al. (1991). Poly(styrene-ethylene oxide) block copolymer micelle formation in water: A fluorescence probe study. *Macromolecules*, *24*(5), 1033–1040.

Wundes, A., Kraft, G. H., Bowen, J. D., Gooley, T. A., & Nash, R. A. (2010). Mitoxantrone for worsening multiple sclerosis: Tolerability, toxicity, adherence and efficacy in the clinical setting. *Clinical Neurology and Neurosurgery*, *112*(10), 876–882.

Xiong, X. Y., Gong, Y. C., Li, Z. L., Li, Y. P., & Guo, L. (2011). Active targeting behaviors of biotinylated pluronic/poly(lactic acid) nanoparticles in vitro through three-step biotin–avidin interaction. *Journal of Biomaterials Science Polymer Edition*, *22*(12), 1607–1619.

Yang, W. Z., Chen, H. L., Gao, F. P., Chen, M. M., Li, X. M., Zhang, M. M., et al. (2010). Self-aggregated nanoparticles of cholesterol-modified pullulan conjugate as a novel carrier of mitoxantronep. *Current Nanoscience*, *6*(3), 298–306.

Yang, X., & Morris, M. E. (2010). Pharmacokinetics and biliary excretion of mitoxantrone in rats. *Journal of Pharmaceutical Sciences*, *99*(5), 2502–2510.

Yu, J. M., Li, Y. J., Qiu, L. Y., & Jin, Y. (2008). Self-aggregated nanoparticles of cholesterol-modified glycol chitosan conjugate: Preparation, characterization, and preliminary assessment as a new drug delivery carrier. *European Polymer Journal*, *44*(3), 555–565.

Zhang, J., Liang, Y. Q., Li, N., Li, X., Hu, R. J., Xing, J. F., et al. (2012). Thermosensitive hydrogel based on poly(ether–ester anhydride) nanoparticle as drug delivery system: Preparation, characterization, biocompatibility. *Colloids and Surfaces B: Biointerfaces*, *96*(0), 56–61.

Zingler, V. C., Nabauer, M., Jahn, K., Gross, A., Hohlfeld, R., Brandt, T., et al. (2005). Assessment of potential cardiotoxic side effects of mitoxantrone in patients with multiple sclerosis. *European Neurology*, *54*(1), 28–33.

Zipser, B., Bradford, J. J., & Hollingsworth, R. I. (1998). Cholesterol and its derivatives, are the principal steroids isolated from the leech species Hirudo medicinalis. *Comparative Biochemistry and Physiology Part C: Pharmacology, Toxicology and Endocrinology*, *120*(2), 269–282.